JOURNAL OF MATERIALS SCIENCE **32** (1997) 2543–2547

The influence of post-bond heat treatment on microstructural development in martensite-forming NiAl–NiTi transient liquid phase bonds employing copper interlayers

W. F. GALE, Y. GUAN
Materials Research and Education Center, Auburn University, Auburn, AL 36849 USA

An investigation is presented of the influence of post-bond heat treatment on microstructural development in transient liquid phase bonds between $L1_0$ martensite-forming Ni–24 at% Al–16 at% Cr and nominally stoichiometric NiTi which transforms to monoclinic (distorted B19 type) martensite. The joints discussed in this article were prepared using 50 μm thick commercial purity copper (99.8 wt% Cu) interlayers and were bonded at 1150 °C for 1 h. The resulting bonds were post-bond heat treated at 1000 °C for times varying between 4 and 12 h and then characterized by edge-on transmission electron microscopy.

The article discusses the formation of Ni_2AlTi (with the $L2_1$ structure) at the bond-line and considers differences in the mode of Ni_2AlTi precipitation between bonding and post-bond heat treatment. Changes in the nature of $Ni_3(Al, Ti)$ precipitation in the NiTi substrate from DO_{24} to $L1_2$ type are examined, as is the homogenization of the matrix of the NiTi substrate adjacent to the joint. Precipitation of Ni_3Al in the NiAl substrate is also considered.

1. Introduction

The joining of intermetallic compounds (in particular NiAl, Ni_3Al and the titanium aluminides) has attracted considerable interest in recent years ([1–4]). Amongst possible joining technologies for intermetallics, transient liquid phase (TLP) bonding [5] offers advantages, such as: tolerance of stable oxide layers on the faying surfaces and a relatively small extent of microstructural disruption. Thus, the TLP bonding of structural intermetallics has been the subject of a number of studies ([2, 3, 6]). The joining of structural intermetallics to conventional metallic systems has also been investigated [7, 8]. In contrast, a similar level of attention has not been paid to the joining of dissimilar intermetallics.

The authors recently presented [9] a microstructural investigation of TLP bonding in a model dissimilar intermetallic system. This system consisted of martensite-forming NiAl–Cr (Ni–24 at % Al–16 at % Cr) and nominally stoichiometric NiTi substrates bonded using 50 μm thick commercially pure copper interlayers (99.8 wt % Cu). This model system was selected because:

1. the system illustrated the key problems of dissimilar intermetallic joining (e.g. formation of stable ternary intermetallics at the bond-line and large compositional disparities between the different constituents of the bonds);
2. both of the substrates examined show shape memory behaviour and hence offer the possibility of producing the shape memory equivalent of the bimetallic strip.

Although the martensite-forming NiAl/Cu/NiTi system was found to be capable of producing fully isothermally resolidified bonds after only a 1 h hold at 1150 °C, a significant difficulty was encountered, as is described below.

Titanium was depleted from the NiTi substrate adjacent to the bond-line in a process associated with the formation of Ni_2AlTi ($L2_1$ type Heusler phase) at the bond centre line. The bulk NiTi substrate underwent transformation from the B2 structure to monoclinic (distorted B19 structure, commonly denoted as B19′) martensite on cooling to room temperature. In contrast, the titanium depleted portion of the NiTi substrate was found to consist of a B2 matrix (containing R-phase precipitation in some regions) with extensive precipitation of both $D0_{24}$ and $L1_2$ type Ni_3Ti. Titanium depletion from the NiTi also has the effect of reducing the liquidus temperature of the NiTi [10]. Titanium depletion continued to the point where, after 2 h holding at 1150 °C, local liquifacation of the outer surface of the NiTi substrate was observed in the titanium depleted region. Given that copper melts at 1083 °C, it was not practicable to reduce the bonding temperature significantly below 1150 °C.

In the present paper, an investigation of post-bond heat treatment at 1000 °C of martensite-forming NiAl–Cr/Cu/NiTi bonds produced by bonding at 1150 °C for 1 h is discussed. The aim of this investigation was to determine the extent to which post-bond heat treatment can be employed to diffuse titanium from the bulk NiTi substrate into the titanium depleted region, without inducing the formation of undesirable microstructural features. Post-bond heat treatments with durations between 4 and 12 h at 1000 °C, followed by furnace cooling to room temperature were investigated.

2. Experimental techniques

NiAl/Cu/NiTi TLP bonds investigated in this paper were fabricated using the following materials:

(a) Ni–24 at % Al–16 at % Cr, prepared by arc melting, with a prior B2 grain size of around 200 μm;

(b) Nominally stoichiometric NiTi (supplied by Shape Memory Applications) with a grain size of around 100 μm;

(c) 50 μm thick commercial purity copper (99.8% Cu) sheet.

Each substrate had a thickness of 2 mm, a faying surface area of 29 mm^2 and a 1000 grit SiC finish.

Joint fabrication was performed under a 5×10^{-4} Pa vacuum atmosphere at a bonding temperature of 1150 °C. Joints were prepared using a holding time at the bonding temperature at 1 h. A heating rate of 2 °C s^{-1} and a cooling rate of 1.5 °C s^{-1} were employed. Post-bond heat treatment was conducted at a temperature of 1000 °C, for times ranging from 4 to 12 h, under conditions similar to those employed during bonding.

The heat treated samples were characterized by edge-on transmission electron microscopy (TEM) using a JEOL JEM 2010 instrument operated at 200 kV together with energy dispersive X-ray spectroscopy (EDS) employing a Link Systems ISIS analyser and an ultrathin window (UTW) detector. Light microscopy (LM) and scanning electron microscopy (SEM) were also performed on the post-bond heat-treated samples. SEM and SEM-based EDS analysis employed a JEOL JSM 840 instrument operated at 20 kV. A Tracor-Northern TN 5500 analyser and UTW detector were utilized for SEM-based EDS analysis. Details of sample preparation procedures are similar to those for as-bonded samples and may be found elsewhere [9].

3. Results and discussion

In the post-bond heat treated samples, the following changes were observed, when compared with the as-bonded samples:

(a) growth of the Ni_2AlTi layer at the bond-line and a change in the growth mechanism of this phase;

(b) alterations in the crystallography and composition of the predominant type of $Ni_3(Al,Ti)$ precipitates in the NiTi substrates;

(c) the eventual disappearance, from the NiTi substrate, of $Ni_3(Al,Ti)$ second phases with increasing post-bond heat treatment duration;

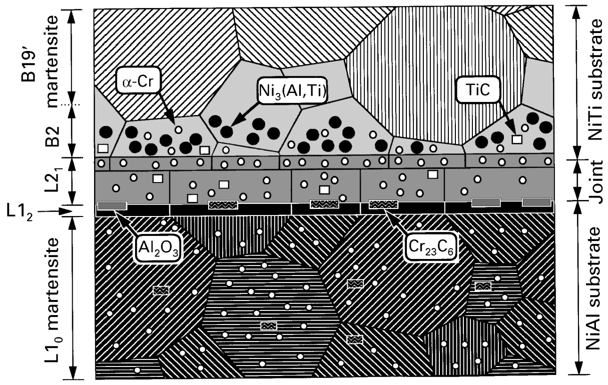

Figure 1 Schematic showing the principal microstructural features developed during post-bond heat treatment of martensite-forming NiAl/Cu/NiTi TLP bonds.

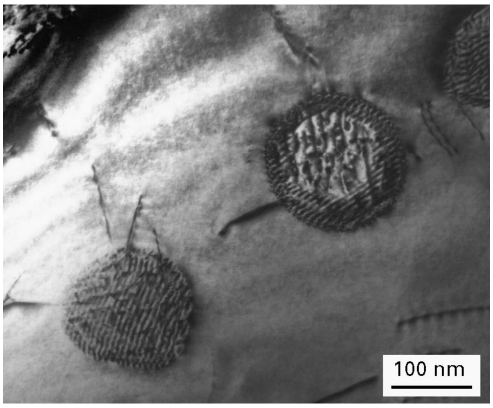

Figure 2 BF image showing spheroidal A2 type α-Cr precipitates present in the joint centre-line $L2_1$ type Ni_2AlTi layer of a sample post-bond heat treated for 6 h at 1000 °C.

(d) contraction of the titanium depleted region of the NiTi substrate with increased post-bond heat treatment times;

(e) precipitation of $Ni_3(Al,Ti)$ in the NiAl substrate after prolonged post-bond heat treatment.

Each of these changes will be discussed in detail.

The microstructures developed during post-bond heat treatment are shown schematically in Fig. 1. Note, the TiC, $Cr_{23}C_6$ and Al_2O_3 phases shown in Fig. 1 were present after bonding [9]. These phases were unchanged by post-bond heat treatment and so are not discussed further here. In all of the post-bond heat treated samples examined in the present work, the copper interlayer (used during bonding) was fully dispersed in the NiAl and NiTi substrates, such that the copper content (even at the bond line) was reduced to below the detection limit of EDS analysis.

3.1 Formation of Ni_2AlTi layers at the bond-line

In the as-bonded samples, a Ni_2AlTi layer was present at the bond-line (Figs 2 and 3). Following post-bond heat treatment, for all of the durations examined (up to 12 h at 1000 °C), the existing Ni_2AlTi remained stable and the formation of an additional Ni_2AlTi layer with a thickness of around 2–5 μm was observed.

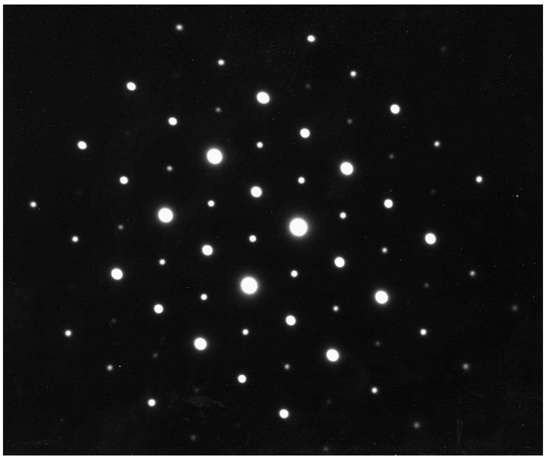

Figure 3 Selected area diffraction pattern with a beam direction of $[1\,1\,0]_{L2_1/A2}$ showing the cube–cube orientation relationship of the A2 type α-Cr precipitate and $L2_1$ type Ni_2AlTi joint centre-line matrix of a sample post-bond heat-treated for 6 h at 1000 °C.

The Ni_2AlTi layer found in the as-bonded samples was epitaxial with the NiAl substrate. However, the new Ni_2AlTi precipitated during heat treatment was observed to be epitaxial with the NiTi substrate. Thus, given that there was no orientation relationship between the (polycrystalline) NiAl and NiTi substrates, a high angle boundary was formed between the new and existing Ni_2AlTi deposits.

$L2_1$ type Ni_2AlTi is formed [11] by additional ordering on the aluminium/titanium sublattice of B2 type Ni(Al, Ti). Thus, the observation that the Ni_2AlTi precipitated during the bonding treatment was epitaxial with the NiAl substrate indicated that this Ni_2AlTi was formed by additional ordering of the NiAl substrate. Conversely, epitaxy between the NiTi substrate and the Ni_2AlTi formed during post-bond heat treatment would result from formation of these Ni_2AlTi deposits by further ordering of the NiTi substrate. However, at the present time, the origins of the change in the growth direction of the Ni_2AlTi layer remain unclear.

3.2 α-Cr precipitation at the bond-line

Precipitation of α-Cr was observed (Fig. 2) within the Ni_2AlTi layer precipitated during post-bond heat treatment. The α-Cr formed with a cube–cube orientation relationship to the Ni_2AlTi (Fig. 3). A similar cube–cube orientation relationship was observed between the B2 matrix and α-Cr precipitated, during bonding, in the titanium-depleted portion of the NiTi substrate. This similarity, in α-Cr/matrix orientation relationship between the Ni_2AlTi layer and the NiTi substrate, would be consistent with the α-Cr observed in the Ni_2AlTi layer having *originally* precipitated in the B2 NiTi phase. In such a case, the α-Cr precipitates would remain incorporated in the $L2_1$ layer after transformation of the B2 phase to the $L2_1$ (Ni_2AlTi) structure. However, the α-Cr observed in the Ni_2AlTi layer consisted entirely of spheroidal precipitates (typically with diameters in the range of 100–300 nm). In contrast, both spheroidal and elongated α-Cr morphologies were observed in the NiTi substrate (in both the as-bonded [9] and post-bond heat-treated conditions). Thus, the α-Cr found in the Ni_2AlTi layer presumably did not result from incorporation of α-Cr inherited from the prior B2 NiTi. Instead, it may have been the case that the α-Cr formed in both the Ni_2AlTi layer and NiTi substrate was precipitated during cooling to room temperature and that chromium remained in solution during both bonding and post-bond heat treatment.

The formation of α-Cr was also observed in both the NiAl substrate and the Ni_2AlTi layer present in the as-bonded samples. These α-Cr precipitates were similar in as-bonded [9] and post-bond heat-treated samples and so are not discussed here.

3.3 Formation of $Ni_3(Al, Ti)$ phases and homogenization of the NiAl and NiTi substrates

After bonding, the titanium depleted region of the NiTi substrate was observed to contain extensive precipitation of Ni_3Ti. Predominantly, this phase was found to posses a $D0_{24}$ type crystal structure (which is the equilibrium Ni_3Ti structure in the Ni–Ti binary system [10, 12]). Some precipitation of $L1_2$ type Ni_3Ti was also observed in as-bonded samples. Post-bond heat treatment was found to result in the disappearance of the $D0_{24}$ type precipitates and replacement by $L1_2$ type precipitates (Figs 4 and 5). These $L1_2$ phases were frequently twinned as is commonly observed in the precipitation of $Ni_3(Al, Ti)$ in NiAl [13, 14]. The following orientation relationship was observed between the B2 NiTi matrix and the $L1_2$ precipitates

$$[1\,1\,1]_{B2} \;//\; [1\,1\,0]_{L1_2}$$

$$(\bar{1}\,1\,0)_{B2} \;//\; (1\,\bar{1}\,\bar{1})_{L1_2}$$

After 6 h holding at 1000 °C, only $L1_2$ type precipitates were observed in the NiTi substrate.

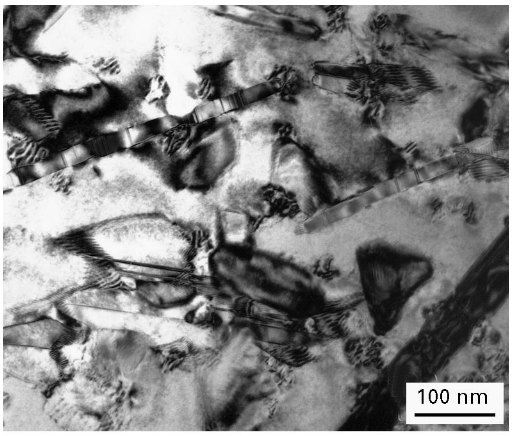

Figure 4 Bright field micrograph showing the precipitation of $L1_2$ type twinned $Ni_3(Al, Ti)$ in the titanium depleted portion of the NiTi substrate of a joint subjected to a 4 h post-bond heat treatment at 1000 °C.

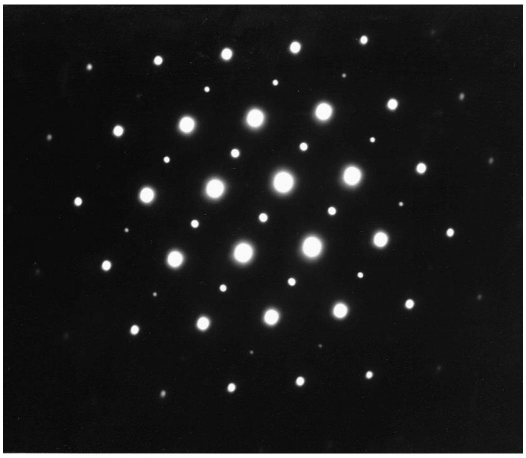

Figure 5 Nano (parallel) beam diffraction pattern with a beam direction of $[1\,1\,0]_{L1_2}$ taken from an $L1_2$ type $Ni_3(Al,Ti)$ precipitate in the titanium depleted portion of the NiTi substrate of a joint subjected to a 6 h post-bond heat treatment at 1000 °C.

In the as-bonded material, both the $L1_2$ and $D0_{24}$ precipitates were found to consist essentially of binary Ni_3Ti. In contrast, post-bond heat treatment was found to result in the entry of aluminium into the precipitates, thus forming $Ni_3(Al,Ti)$. The Ni_3Al phase formed in the binary Ni–Al system has the $L1_2$ crystal structure [10, 12]. Thus replacement of titanium by aluminium would be expected to result in stabilization of the $L1_2$ phase over the $D0_{24}$ structure. However, a mechanism leading to the formation of essentially aluminium-free Ni_3Ti with an $L1_2$ type structure in the as-bonded material remains unclear ($L1_2$ type metastable Ni_3Ti is usually precipitated in an A1 type disordered Ni–Ti matrix [15] rather than in B2 NiTi).

With increasing holding at the 1000 °C post-bond heat treatment temperature, contraction of the titanium depleted region in the NiTi substrate was observed. After 12 h holding at 1000 °C, diffusion of titanium from the bulk NiTi into the region of the NiTi substrate adjacent to the joint was sufficient to suppress entirely the formation of $Ni_3(Al,Ti)$. However, a region extending (from the interface with Ni_2AlTi layer) around 10 μm into the NiTi substrate retained the B2 structure on cooling to room temperature. In contrast, the remainder of the substrate was transformed to a (distorted B19 structure) monoclinic martensite. The composition of the B2 layer could not, within the capabilities of EDS analysis, be reliably distinguished from that of the bulk NiTi substrate. Thus, any residual compositional inhomogeneity in the NiTi substrate was relatively small, although still sufficient to locally suppress the martensite start (M_s) temperature to below room temperature.

Ideally, post-bond heat treatment would be continued until the titanium depleted region in the NiTi substrate is removed entirely, such that the whole of the NiTi substrate undergoes martensitic transformation on cooling to room temperature. In practice, however, the maximum post-bond heat treatment that could be gainfully employed (with the compositional and process conditions employed in the present work) was limited to a duration of less than 12 h at 1000 °C. The factor that was found to limit the useful length of post-bond heat treatment was damage to the NiAl substrate induced by the diffusion of aluminium from this substrate into the joint region. After 12 h at 1000 °C, aluminium loss from the NiAl substrate was sufficient to induce the precipitation of $L1_2$ structured Ni_3Al (containing a small amount of titanium) close to the interface between the NiAl substrate and the bond-line Ni_2AlTi. The Ni_3Al formed a near continuous layer which typically possessed a thickness of around 500 nm. The $L1_0$ martensite matrix of the NiAl substrate and the $L1_2$ type Ni_3Al layer were orientation related such that, if the tetragonal distortion of the $L1_0$ phase was not present, the $L1_0$ and $L1_2$ phases could be described as "cube–cube". From this observation, the original B2 (NiAl substrate) to $L1_2$ (Ni_3Al layer) orientation relationship can be ascertained as follows. The precipitation of A2 type α-Cr in B2 type NiAl invariably occurs with a cube–cube orientation relationship between precipitate and matrix [16–18]. Thus, the observed $L1_0$ martensite to α-Cr orientation relationship

$$[1\,1\,0]_{L1_0} \;//\; [0\,0\,1]_{\alpha\text{-Cr}}$$

$$(1\,\bar{1}\,1)_{L1_0} \;//\; (1\,\bar{1}\,0)_{\alpha\text{-Cr}}$$

would be expected to be the same as the orientation relationship between the B2 parent and $L1_0$ product of the martensitic transformation of the NiAl substrate's matrix. Hence, the orientation relationship between the (original) B2 matrix of the NiAl substrate and the $L1_2$ type Ni_3Al would have been such that

$$[0\,0\,1]_{B2} \;//\; [1\,1\,0]_{L1_2}$$

$$(1\,\bar{1}\,0)_{B2} \;//\; (1\,\bar{1}\,1)_{L1_2}$$

It would seem reasonable to assume that the $L1_2$ structured layer was formed prior to the transformation of the B2 matrix of the NiAl substrate to $L1_0$ martensite. However, it is not possible, based on the observations made in the present work, to ascertain whether the $L1_2$ type Ni_3Al layer formed during holding at the 1000 °C post-bond heat treatment temperature or in the early stages of cooling back to room temperature.

4. Conclusions

An investigation has been undertaken into the influence of post-bond heat treatment on microstructural development in martensite forming NiAl–Cr/Cu/NiTi transient liquid phase bonds. As a result of this investigation, the following conclusions have been drawn:

1. The formation of $L2_1$ structured Ni_2AlTi was observed at the bond-line after post-bond heat treatment. This layer was epitaxial with the NiTi substrate, unlike an adjacent layer of Ni_2AlTi, remaining from the bonding treatment, which formed epitaxially with the NiAl substrate. α-Cr precipitation was observed within the Ni_2AlTi layer formed during post-bond heat treatment. This α-Cr appeared to result from

rejection of chromium directly from the Ni_2AlTi, rather than incorporation of existing α-Cr precipitates during growth of the Ni_2AlTi layer.

2. Post-bond heat treatment was observed to modify the character of $Ni_3(Al, Ti)$ precipitates formed in the NiTi substrate adjacent to the bond-line. In the as-bonded condition, essentially binary Ni_3Ti was produced and the predominant precipitate type was $D0_{24}$, although a significant number of $L1_2$ type phases were also present in the NiTi substrate. Following post-bond heat treatment $Ni_3(Al, Ti)$ precipitates were observed and the entry of aluminium into these precipitates correlated with a change in the predominant precipitate type from $D0_{24}$ to $L1_2$.

3. The formation of $Ni_3(Al, Ti)$ precipitates in the NiTi substrate was associated with transfer of titanium from the NiTi substrate to the bond-line during bonding. Post-bond heat treatment resulted in diffusion of titanium from the bulk NiTi substrate to the titanium depleted region adjacent to the bond-line. After 12 h holding at 1000 °C, sufficient titanium transfer occurred to prevent the formation of $Ni_3(Al, Ti)$ within the NiTi substrate. However, the M_s temperature of the portion of the NiTi substrate immediately adjacent to the bond-line remained below room temperature.

4. Post-bond heat treatment for 12 h at 1000 °C resulted in significant transfer of aluminium from the NiAl substrate to the bond-line and this, in turn, led to the formation of an $L1_2$ type Ni_3Al layer at the interface between the NiAl substrate and the joint centreline Ni_2AlTi.

Acknowledgements

The research described in this paper was supported by the NSF–EPSCoR programme "Smart Materials for Transport Control". The instrumentation employed for this work was funded by the NSF–ARI programme.

References

1. M. C. MAGUIRE, G. R. EDWARDS and S. A. DAVID, *Weld. J.* (*Res. Suppl.*) **71** (1992) 231.
2. T. J. MOORE and J. M. KALINOWSKI, *MRS Symp. Proc.* **288** (1993) 1173.
3. M. J. STRUM and G. A. HENSHALL, in "Advanced joining technologies for new materials II", edited by N. F. Flore and J. O. Stiegler, (AWS, Miami, FL, 1994) p. 76.
4. P. YAN and E. R. WALLACH, *Intermetallics* **1** (1993) 83.
5. D. S. DUVALL, W. A. OWCZARSKI and D. F. PAULONIS, *Weld. J.* **53** (1974) 203.
6. P. YAN, PhD Thesis, University of Cambridge, UK, 1993.
7. W. F. GALE and S. V. OREL, *Metall. Mater. Trans. A*, **27A** (1996) 1925.
8. W. F. GALE and Y. GUAN, *ibid.* **27A** (1996) 3621.
9. *Idem.*, *J. Mater. Sci.* in press.
10. T. B. MASSALSKI (ed.), "Binary alloy phase diagrams", (ASM, Metals Park, OH, 1986).
11. P. SHEN, D. GAN and C. C. LIN, *Mater. Sci. Engng.* **78** (1986) 163.
12. P. VILLARS and L. D. CALVERT, "Pearson's handbook of crystallographic data for intermetallic phases", vol. 2, (ASM, Metals Park, OH, 1985).
13. W. F. GALE, *Intermetallics*, **4** (1996) 585.
14. R. YANG, J. A. LEAKE and R. W. CAHN, *J. Mater. Res.* **6** (1991) 343.
15. A. J. ARDELL, *Metall. Trans.* **1** (1970) 525.
16. W. F. GALE and J. E. KING, *J. Mater. Sci.* **28** (1993) 4347.
17. R. YANG, J. A. LEAKE and R. W. CAHN, *Phil. Mag. A* **65** (1992) 961.
18. R. D. FIELD, D. F. LAHRMAN and R. DAROLIA, *Acta Metall. Mater.* **39** (1991) 2961.

Received 12 July
and accepted 23 October 1996